

Supplementary Information

Mechanochemical cocrystallization to improve the physicochemical properties of chlorzoxazone

Parag Roy, Animesh Ghosh,*

Department of Pharmaceutical Sciences & Technology, Birla Institute of Technology, Mesra, Ranchi, Jharkhand, India.

* Email: aghosh@bitmesra.ac.in

Tables:

- S1.** Results of screening of the coformers for obtaining cocrystals.
- S2.** Hydrogen bonding distances and angles for CHZ-PA cocrystal.
- S3.** Solubilities of CHZ and CHZ-PA Cocrystal in different media.

Figures:

- S1.** Oxazolone rings of CHZ forming Homosynthon Dimers.
- S2.** Thermal ellipsoid structure of CHZ-PA Cocrystal.
- S3.** PXRD patterns of the Mechanochemically synthesized cocrystal and simulated pattern.
- S4.** Combined thermal investigation of the CHZ-PA cocrystal (DSC and TGA).
- S5.** PXRD patterns of the residual solids of the CHZ-PA cocrystals.
- S6.** Chromatogram of the 13-week accelerated stability sample obtained in HPLC.
- S7.** Laminated tablets of CHZ.
- S8.** Crystal Structure of CHZ viewed down reciprocal to a -axis.
- S9.** Presence of a slip-plane system in CHZ-PA cocrystal.

Table S1: Results of screening of the coformers for obtaining cocrystals.

| Coformer | Molar ratio | Observation |
|-----------------------------|--------------------|---|
| Picolinic Acid | 1:1, 1:2, 2:1 | Changes in the PXRD pattern observed using acetonitrile. Cocrystal (1:1) obtained in ethyl acetate. |
| Fumaric Acid | 1:1, 1:2, 2:1 | Eutectic |
| Trimesic Acid | 1:1, 1:2, 2:1 | Eutectic |
| Glutaric Acid | 1:1, 1:2, 2:1 | Eutectic |
| Nicotinic Acid | 1:1, 1:2, 2:1 | Eutectic |
| Malonic Acid | 1:1, 1:2, 2:1 | Eutectic |
| Benzoic Acid | 1:1, 1:2, 2:1 | Eutectic |
| Gentisic Acid | 1:1, 1:2, 2:1 | Eutectic |
| <i>p</i> -aminobenzoic acid | 1:1, 1:2, 2:1 | Eutectic |
| Mandelic Acid | 1:1, 1:2, 2:1 | Eutectic |
| Succinic Acid | 1:1, 1:2, 2:1 | Eutectic |
| Maleic Acid | 1:1, 1:2, 2:1 | Eutectic |
| Malic Acid | 1:1, 1:2, 2:1 | Eutectic |

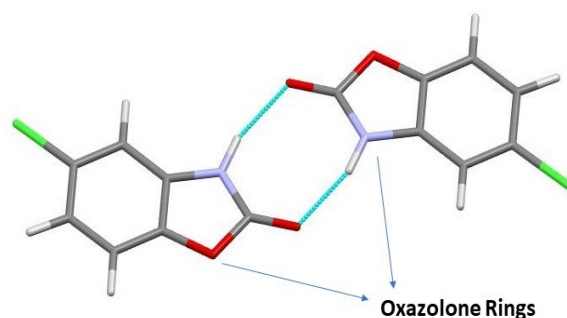
Optimization of the parameters: The grinding parameters were optimized by taking the API and coformers in different stoichiometric ratios. There were no changes observed in neat grinding; therefore, liquid assisted grinding was performed with acetonitrile, methanol, tetrahydrofuran, ethyl acetate as LAG solvents. The RPM of the planetary ball mill was kept constant at 500 rpm, and the number of balls (10 stainless steel balls, $\phi = 0.5$ mm) was also kept constant throughout all the screening experiments. Initially, the grinding time was also kept constant to 30 mins. In Initial experiments, the amount of solvents taken was $1000 \mu\text{L}$ ($\eta = 1 \mu\text{L mg}^{-1}$). Upon confirmation of the formation of CHZ-PA cocrystal by ACN as the LAG solvent, the value of η was altered with respect to the volume of solvents to optimize the parameters. In $\eta = 0.5 \mu\text{L mg}^{-1}$, the formulated product was also confirmed by PXRD, and the PXRD pattern was exactly matching with the previous one ($\eta = 1 \mu\text{L mg}^{-1}$). To optimize the milling time, mechanochemical studies were performed at various time points (5, 10, 15, 30 and 45 mins) (Figure 4). The formation of cocrystal was confirmed at 30 mins and the PXRD pattern of the material after 45 mins of grinding was exactly matching with the PXRD pattern of material after 30 mins of grinding.

Table S2: Hydrogen bonding distances and angles for CHZ-PA cocrystal.

| D—H...A | D...H (Å) | H...A (Å) | D...A (Å) | ∠D—H...A (deg) | Symmetry code |
|------------|-----------|-----------|-----------|----------------|---------------|
| N2-H6...O1 | 0.860 | 2.643 | 3.436(2) | 153.98 | x,y,z |
| N2-H6...O2 | 0.860 | 2.046 | 2.819(2) | 149.13 | x,y,z |
| C1-O1...H1 | 1.240(2) | 1.85(2) | 3.04(2) | 159.6(6) | 2-x,-y,1-z |
| N1-H1...O1 | 0.87(2) | 1.85(2) | 2.667(2) | 156(2) | 2-x,-y,1-z |
| C1-O2...H6 | 1.236(2) | 2.046 | 2.583 | 100.9 | x,y,z |
| C1-O1...H6 | 1.240(2) | 2.643 | 2.583 | 73.63 | x,y,z |

Table S3: Solubilities of CHZ and CHZ-PA Cocrystal in different media (n=3). Values are stated as Mean ± S.D.

| Media | CHZ (mg/mL) Equilibrium Solubility | CHZ-PA Cocrystal (mg/mL) Equilibrium Solubility |
|--------|---------------------------------------|--|
| Water | 0.2587 ± 0.018 | 0.5467 ± 0.011 |
| pH 1.2 | 0.2562 ± 0.016 | 0.5540 ± 0.014 |
| pH 4.5 | 0.2699 ± 0.008 | 0.5662 ± 0.007 |
| pH 6.8 | 0.2767 ± 0.005 | 0.5569 ± 0.017 |
| pH 7.4 | 0.2867 ± 0.012 | 0.5673 ± 0.015 |

**Figure S1:** Oxazolone rings of CHZ forming Homosynthon Dimers. Hydrogen bonds depicted as blue dashed lines. (As represented in Mercury⁵³)

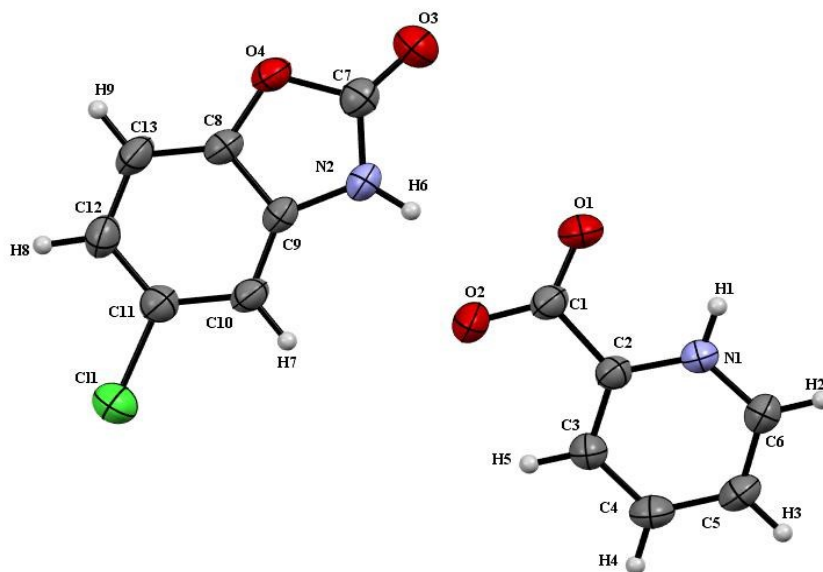


Figure S2: Thermal ellipsoid structure of CHZ-PA Cocrystal, including atomic labeling at 50% probability level. (As represented in Mercury⁵³).

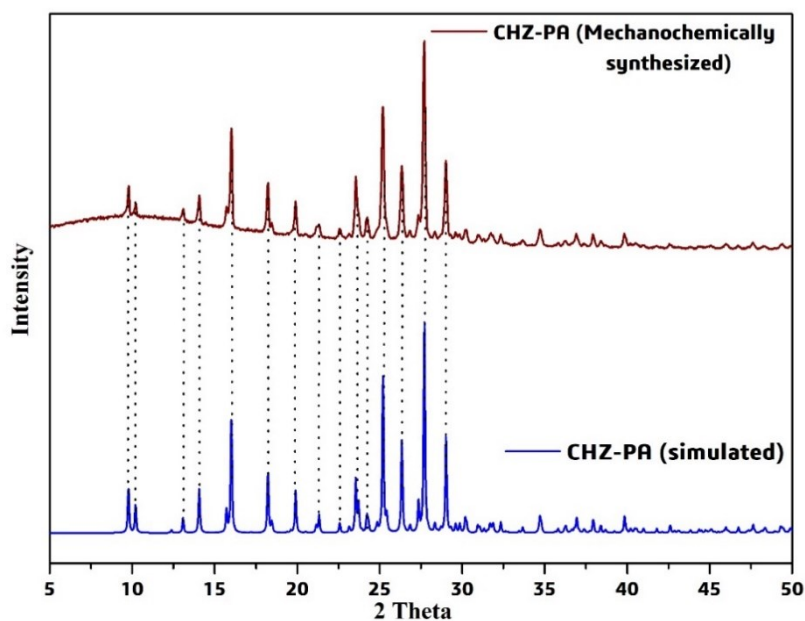


Figure S3: Overlaid PXRD patterns of the Mechanochemically synthesized cocrystal and simulated pattern obtained from the SCXRD data to check the presence of impurities.

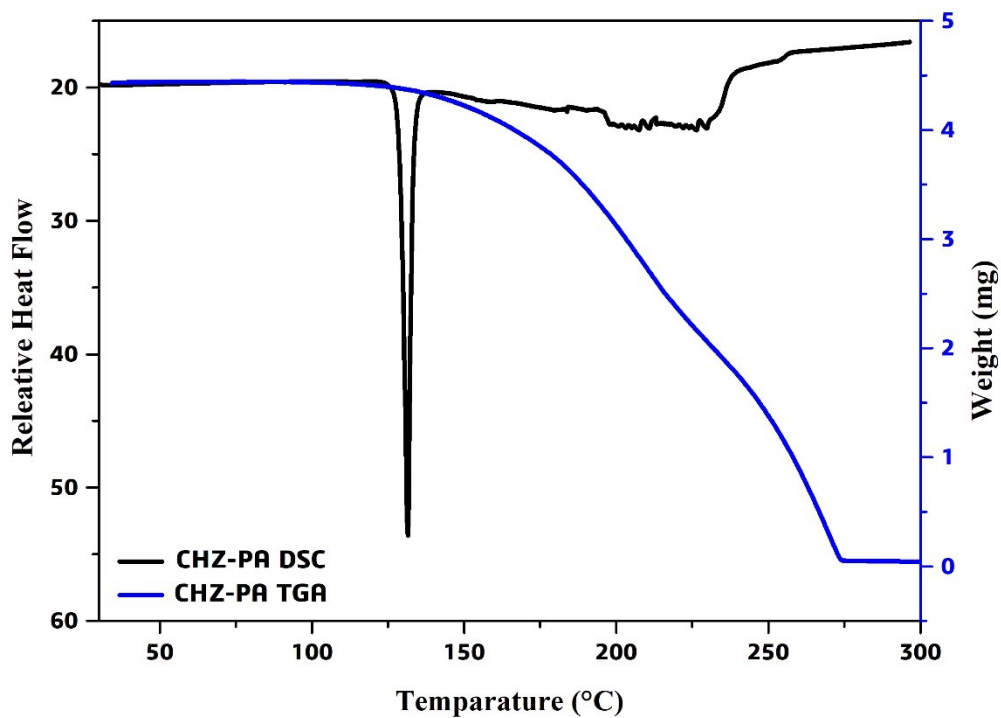


Figure S4: A combined thermal investigation of the CHZ-PA cocrystal (DSC and TGA).

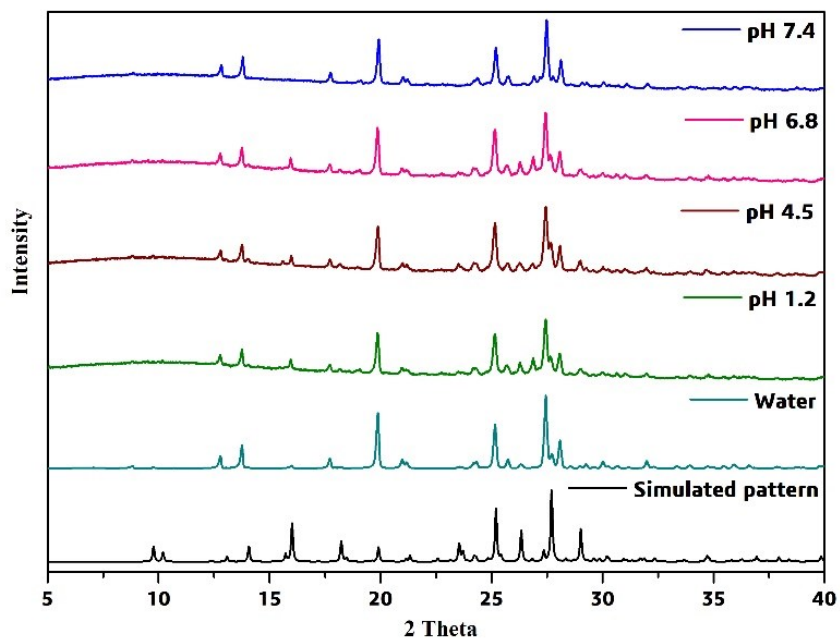


Figure S5: PXRD patterns of the residual solids of the CHZ-PA cocrystals obtained after equilibrium solubility experiments.

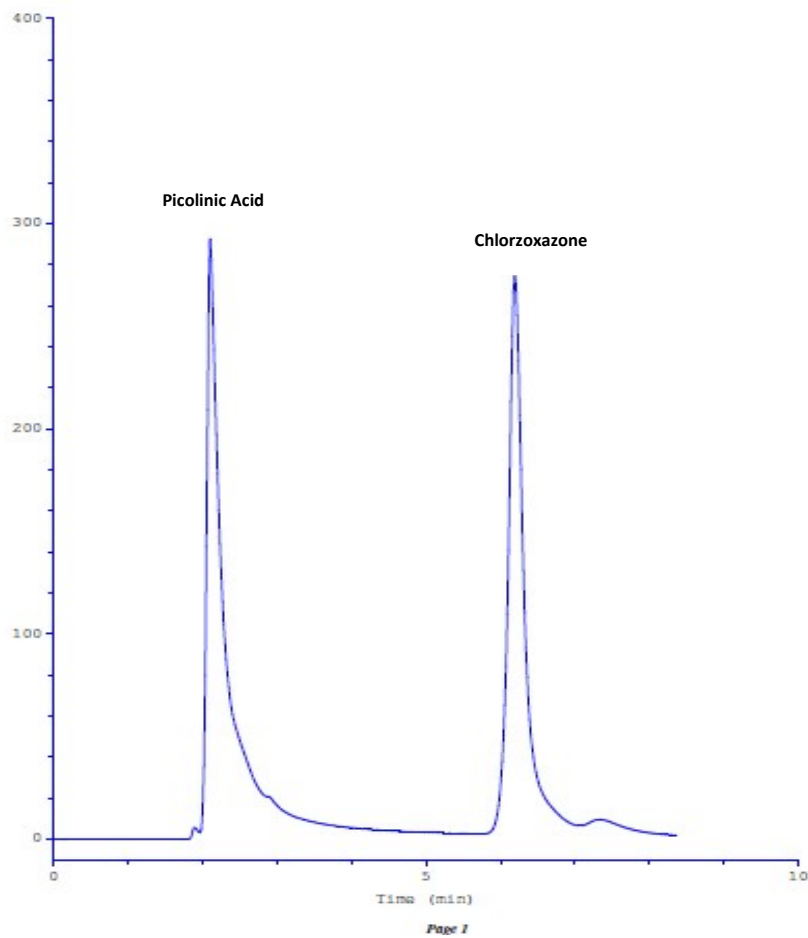


Figure S6: Chromatogram of the 13-week accelerated stability sample obtained in HPLC.



Figure S7: Laminated tablets of CHZ.

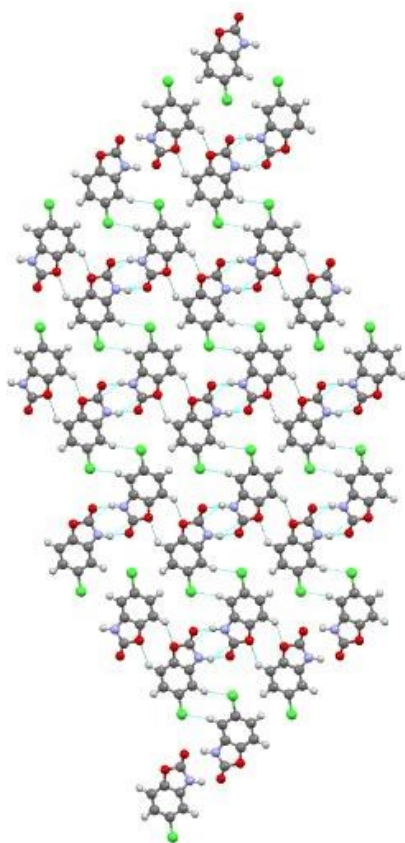


Figure S8: Crystal Structure of CHZ as reported by S. ide and A. Topa q .³⁶ Viewed down reciprocal to a -axis. (As represented in Mercury⁵³).

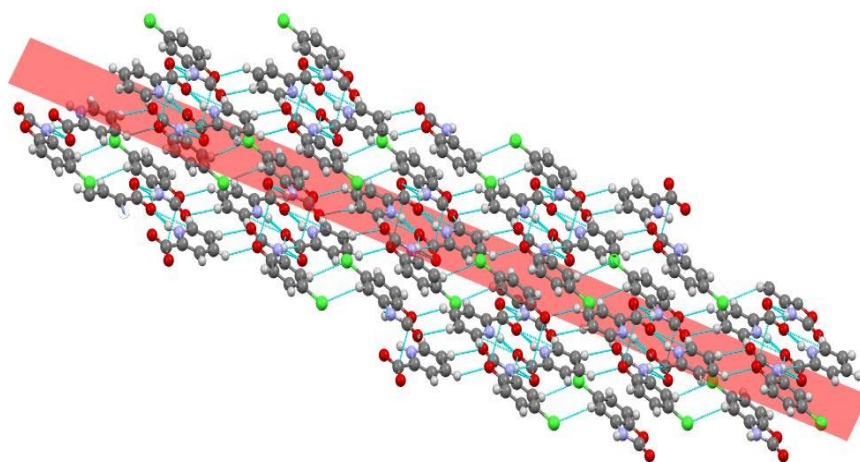


Figure S9: Presence of a slip-plane system in CHZ-PA cocrystal due to the presence of auxiliary intermolecular interactions. Viewed along the b-axis. (As represented in Mercury⁵³).